POPULAR SUMMARY

for

Estimating the Soil Temperature Profile from a Single Depth Observation: A Simple Empirical Heatflow Solution

Thomas Holmes, Manfred Owe, and Richard de Jeu

A simple model is developed, to derive the surface temperature profile for a bare soil from a single near surface observation. It is shown that a number of commonly used theoretical modeling approaches do not work well when extreme variations in temperature occur near the surface. The reason for this is that these approaches do not properly characterize the near-surface heat that results from the incoming solar energy. The new model is developed and validated with two independent data sets from different soils and under a range of meteorological conditions. Many experimental and operational soil temperature data sets have been compiled at a variety of spatial and temporal scales. However, a major problem with these datasets, is that the observations are typically not measured at the same depth. The proposed modeling approach can help unify these datasets by expressing these measurements at a common depth. This work may contribute to many different types of global environmental monitoring research and activities.

Estimating the Soil Temperature Profile from a Single Depth Observation: A Simple Empirical Heatflow Solution

Thomas Holmes (1)
Manfred Owe (2)
Richard de Jeu (1)

(1)   Dept. of Geo-Environmental Sciences
        Vrije Universiteit Amsterdam
        De Boelelaan 1085
        1081 HV Amsterdam
        The Netherlands

(2)   Hydrological Sciences Branch/614.3
        NASA Goddard Space Flight Center
        Greenbelt, MD, USA

Corresponding author address:

Manfred Owe
Mail Code 614.3
NASA Goddard Space Flight Center
Greenbelt, MD 20771, USA

Telephone: +1-301-614-5783
FAX: +1-301-614-5808
Email: Manfred.Owe@nasa.gov

1   **Abstract**

2   Two data sets of experimental field observations with a range of meteorological conditions are

3   used to investigate the possibility of modeling near–surface soil temperature profiles in a bare

4   soil. It is shown that commonly used heat flow methods that assume a constant ground heat flux

5   can not be used to model the extreme variations in temperature that occur near the surface. This

6   paper proposes a simple approach for modeling the surface soil temperature profiles from a

7   single depth observation. This approach consists of two parts: 1) modeling an instantaneous

8   ground flux profile based on net radiation and the ground heat flux at 5cm depth; 2) using this

9   ground heat flux profile to extrapolate a single temperature observation to a continuous near-

10   surface temperature profile. The new model is validated with an independent data set from a

11   different soil and under a range of meteorological conditions.

1. INTRODUCTION

1

2   Surface temperature is an important parameter for many research applications that

3 encompass the air–soil interface, but unlike other environmental parameters such as air

4 temperature and precipitation, soil temperature is rarely measured on a regular basis at

5 meteorological and climate stations. Most historical soil temperature data bases have been

6 compiled from various field experiments, and as a result, these data are usually limited in both

7 duration and spatial coverage. Furthermore, the depth at which soil temperature is measured

8 typically varies according to the specific application for which the measurement campaign was

9 designed. Soil temperature profiles frequently exhibit steep gradients, which may be especially

10 steep near the surface. Because of the inherent differences associated with different observational

11 data sets, it is often difficult to make direct comparisons between them, and as a result, the direct

12 application of these data to other research activities is not always straightforward. For example,

13 many energy balance applications have a distinct requirement for surface temperature, such as in

14 the calculation of latent and sensible heat fluxes. However, surface temperature is difficult to

15 measure on a sustained basis with embedded monitoring devices such as thermistors. The

16 shallowest depth at which the temperature is measured typically varies between 0 and 5

17 centimeters. However, near-surface measurements (< 1 cm) are often corrupted because the

18 precise depth of the emplaced measuring device is difficult to maintain, usually due to weather-

19 related disturbances.

20   Several models have been developed to supplement limited temperature data [*Van Wijk*

21 *and De Vries,* 1963; *Camillo,* 1989; *Cuaraglia,* 2001; *Elias et al.,* 2004]. When properly

22 implemented, these models can be used to extrapolate soil profile temperatures with reasonable

23 accuracy from a single subsurface measurement. *Van Wijk and De Vries* [1963] fitted sine waves

1   with diurnal and seasonal periods to the observed temperature cycles at two depths. The

2   amplitude of these temperature oscillations decreases exponentially with depth. Others have built

3   on Van Wijk's fourier series to broaden the scope of that model. *Camillo* [1989] combined the

4   fourier series with a simple model of time dependent surface soil heat flux. This model was fitted

5   to observations to derive five model parameters, but this makes it difficult to apply on a broader

6   scale. More recently, *Elias et al.* [2004] improved on the Van Wijk model by introducing a

7   correction for the temporal variation of daily amplitude. This addition makes the model better

8   suited for inter-seasonal timescales. A different approach was used by *Guaraglia* [2001], who

9   used electrical modeling to predict temperature and heat flow at one depth from solar radiation.

10   However, it has been observed, that these models tend to break down under certain

11   environmental conditions, especially during midday periods, when incoming radiation is at a

12   peak. The standard solutions to the heat flow equations are frequently unable to describe the

13   temperature fluctuations to an acceptable accuracy, especially when either the input observation

14   or the calculated value is at or near the surface. The near-surface energy balance is not well

15   described in the model, causing significant systematic errors in the temperature calculations.

16   A physically–based model that can calculate relatively accurate near–surface soil

17   temperature profiles from a single observation can be an extremely useful tool for the reasons

18   mentioned above. In addition, Earth Observation Systems (*e.g.* Aqua/Terra MODIS, ENVISAT,

19   ASTER, Landsat TM) provide spatially distributed land surface temperature products. Reliable

20   temperature profiles derived from this model in combination with these satellite products may be

21   an important contribution to global energy and water balance studies.

22   This paper proposes an approach to model near–surface soil temperature profiles in a

23   bare soil, using only a single temperature measurement, net radiation, and an estimate of the soil

1   moisture content. Two experimental datasets with near-surface temperature measurements within

2   the first centimeter of the soil were studied in the development of this model.

3

4   **2. BACKGROUND**

5   Many soil temperature profile numerical modeling approaches are based on the solutions

6   to the heat flow equations developed by *Van Wijk and De Vries* [1963]. These equations can be

7   summarized by starting with the basic energy balance at the land surface. The steady-state heat

8   balance equation is given by:

9                          $R_n = H + LE + G$ (1)

10 where H is the sensible heat flux, LE is the latent heat flux, and G is the soil heat flux or the

11 vertical transport of heat in the soil column. All components are given in W/m^2. At the air–soil

12 interface of a bare surface, the soil heat flux may be considered equal to the net radiation. As the

13 energy moves downward into the soil, it is further redistributed and some is converted to latent

14 and sensible heat. At a certain depth below the surface the sensible and latent heat flux become

15 zero, and the total energy flux in the soil becomes equal to the soil heat flux (see Figure 1). It is

16 reasonable to assume that the latent and sensible heat fluxes are negligible below a depth of 5

17 cm. Below this depth, the change in temperature δT (K) over a given interval δz (m) is then

18 governed only by heat conduction. The soil heat flux can be described according to Fourier's

19 Law

20                          $G = - \lambda \cdot \delta T / \delta z$ (2)

21 where λ ($Wm^{-1}K^{-1}$) is the soil thermal conductivity and z is the depth (m). The diurnal and

22 seasonal variations in soil temperature may be described by sine waves, varying around an

23 average temperature, T_a (K). T_a is considered constant with depth, due to the assumption of heat

1 conservation. Theoretically, this is true over the long term. However, it is not true in the short

2 term, for the same reason that the soil heat flux does not always equal zero over a 24 hour period.

3 If this were true, the soil temperature would not change over the course of season.

4 Under ideal conditions, the amplitude of the temperature wave is at a maximum at the

5 soil surface and decreases with depth. The maximum temperature also occurs shortly after solar

6 noon at the surface, but lags in time with increasing depth. Based on these assumptions, the

7 solution to the heat flow equations for the diurnal cycle is given as [V*an Wijk and De Vries,*

8 1963]

9 $$T_{(z,t)} = T_a + A \cdot \exp(-z/D) \cdot \sin(\omega \cdot t - z/D + \varphi) \tag{3}$$

10 $$D = \sqrt{(2K/\omega)} \tag{4}$$

11 $$\omega = 2\pi/\tau \tag{5}$$

12 where A (K) is the amplitude of the daily surface temperature fluctuations, t(s) is the time, z is

13 the depth (m) (positive downwards), and φ is a phase constant. The damping depth, D (m), is the

14 depth at which the amplitude of surface temperature oscillations is reduced by e^{-1}. The thermal

15 diffusivity, K (m^2/s), is assumed to be constant with depth, ω (s^{-1}) is the angular frequency, and τ

16 (s) is the period of the wave. The same approach can be applied to the seasonal temperature cycle

17 in the soil, but for shallow depths (z<10cm) the seasonal oscillations are insignificant compared

18 to the diurnal oscillations.

19

20 ## 3. FIELD OBSERVATIONS

21 Soil temperature, soil moisture, ground heat flux, and radiation measurements from two

22 experimental field studies were used in this study. The first data set is from the U.S. Department

23 of Agriculture Water Conservation Laboratory in Phoenix, Arizona. These data were collected

1   during a three-week dry-down experiment on a loam soil in 1971 [*Jackson, 1973; Idso et al.,*

2   *1975*]. The second data set was obtained during an 8 month field experiment conducted on a clay

3   soil at the Wageningen Agricultural University meteorological station in Wageningen, The

4   Netherlands [*De Jeu et al.,* 2003, *www.met.wau.nl*]. Both experiments measured soil temperature

5   and moisture at multiple points within the surface profile, with the shallowest near-surface

6   observation within the first centimeter. Measurements were made at 30 minute intervals in each

7   case. This data was supplemented with net radiation and ground heat flux measurements. At the

8   Phoenix site the ground heat flux was measured at 5 cm depth, at the Wageningen site at 2 cm

9   depth. The Phoenix dataset has a higher vertical resolution of temperature and moisture

10   measurements than the Wageningen dataset, and therefore it was chosen as the calibration

11   dataset. The Wageningen data is used to validate the model's performance under somewhat

12   different soil and environmental conditions.

13

4. MODELING APPROACH

15   **4.1 Basic Soil Temperature Model (Model A)**

16   The Van Wijk heatflow equations (Equation 3–5) can be used to model soil temperature

17   at a depth, z_1, from a temperature measured at a depth z_0 and time t_0. From temperature

18   observations with a temporal resolution of 30 minutes, the 24 hour moving average temperature

19   T_{am} is calculated. The diurnal temperature departures from the moving average ($\delta T_D(z_0,t_0)$)

20   described by the sine function in Equation 3 is then given by

21                              $$\delta T_D(z_0,t_0) = T(z_0,t_0) - T_{am} \tag{6}$$

22   The temperature at depth z_1 can then be modeled by correcting the $\delta T_D(z_0,t_0)$ for the exponential

23   change in amplitude

1

2
$$T(z_1, t_1) = T_{am} + \delta T_D(z_0, t_0) \cdot \exp((z_0 - z_1)/D(t_0)) \tag{7}$$

3   Because of the phase shift of the diurnal temperature cycle between two depths, this model does

4   not calculate the temperature for the same time, t_0, as the initial observation. The time, t_1, is

5   subsequently given by

6
$$t_1 = t_0 - ((z_0 - z_1) / D(t_0)/\omega) \tag{8}$$

7   This means that t_1 is earlier than t_0 if $z_1 < z_0$, and later if $z_1 > z_0$. However, if the temporal

8   resolution of the measurements is at least one hour, then the calculated temperature can be

9   interpolated accurately at the original observation time.

10   The damping depth, $D(t_0)$, is calculated according to Equation 4. The diffusivity, K, is

11   calculated from soil properties and the water content θ (m^3/m^3) [*Johansen*, 1975; *Peters-Lidard*

12   *et al.*, 1998]. This makes the damping depth variable with time (and depth if profile data is

13   available). Ideally, water content should be available at several depths within the first

14   centimeters, so that the soil moisture profile is sufficiently represented. When soil moisture

15   profile data is lacking, it is somewhat important that the average soil moisture is reasonably

16   approximated. In this study, the observed soil moisture profile was used to calculate the

17   diffusivity for each layer with temperature measurements.

18

19   **4.2 Model A Results**

20   The Phoenix data set has a relatively dense vertical network of moisture and temperature

21   measurements in the surface profile, and is used to test Model A. Model simulations were

22   performed for 0100 hours and 1300 hours, as these time periods represent two widely differing

23   conditions; a relatively uniform temperature profile and a warming profile during the period of

1   near-peak solar radiation. Soil moisture profiles for these time periods are also provided to assist

2   in the interpretation of the results (Figure 2a). While some drying is observed in the upper profile

3   during the day, the moisture profiles are essentially the same below 2 cm. The simulated

4   temperature profiles are derived from 8 cm input temperature observations and compared to the

5   measured values (Figure 2b). Model simulations for the nighttime data are seen to correspond

6   well with the observations over the entire profile. However, model simulations during midday

7   clearly underestimate the observations. Although the simulations compare reasonably well to

8   observations within the first several cm of the input value, the difference becomes increasingly

9   larger as one approaches the soil surface.

10   These results are further supported when we examine several four day time series of

11   diurnal temperature measurements and simulations at different depths (Figure 3). Each plot

12   shows an input temperature, modeled temperature, and the observation at the modeled depth.

13   Results of upward model simulations (where $z_0 = 5$ cm and $z_1 = 2$ cm) and downward

14   simulations (where $z_0 = 2$ cm and $z_1 = 5$ cm) are illustrated (Figures 3a and 3b). These time

15   series simulations compare well with observations during the four-day period, although the

16   model slightly underestimates the temperature gradient at midday by approximately 2 K and 1K

17   in the upward and downward simulations, respectively. RMS errors of 0.7 K and 0.5 K were

18   found for the full diurnal 14-day period, while RMS errors of 0.9 and 0.4 were found for the time

19   of greatest daily deviation (~1300 hours). However, model simulations from 5 cm to 0.5 cm and

20   0.5 cm to 5 cm (Figures 3c and 3d) illustrate conditions which result in a more extreme

21   breakdown in model performance. In the upward simulation, the modeled temperature

22   underestimates the observation by as much as 10 K during midday, while in the downward

23   simulation the modeled temperature overestimates by as much as 6 K. RMS errors for the full

1   diurnal 14-day period are 3.4 K and 2.3 K respectively, while the RMS errors for the simulations

2   at 1300 hours are 6.9 K and 4.1 K.

3   These errors are due, in part, because one of the main assumptions of the Van Wijk

4   heatflow parameterization, that no heat is generated in the soil or converted into other forms of

5   energy, such as latent or sensible heat, is not valid most of the time. This is especially the case at

6   the surface or near-surface layers, when the difference between z_0 and z_1 is large, or other

7   conditions where the soil heat flux may change significantly. A direct follow-on of this

8   assumption would be that the ground heat flux remains constant with depth. We know that this is

9   not true. Furthermore, it would then also follow that the average temperature for each soil layer

10   is the same. Theoretically, this is true on an annual basis; however, it is probably not true on a

11   daily or seasonal time scale. The differences in mean temperature between depths is not great,

12   but will exist because the heating and cooling cycles, although gradual, occur at different rates

13   within the profile during their respective seasons.

14   At the air-soil interface, the downward soil heat flux is approximately equal to the net

15   radiation. This energy is then directed downward into the soil, at a rate that is dependent upon

16   the ability of the soil to conduct heat. As this heat energy is directed downward, some is

17   transformed and redirected upward, eventually exiting the soil in the form of latent and sensible

18   heat. For a schematic representation of these processes, see Figure 3. Moreover, when the

19   incoming energy exceeds the soil's ability to conduct heat downward, the energy will be stored

20   temporarily and the soil temperature will increase. The relative distribution of these flux rates

21   within the soil is largely determined by the physical properties of the soil medium, e.g. soil

22   particle density, porosity, and especially soil moisture content. A simple ground heat flux

1   parameterization is introduced to account for this redistribution of fluxes in the soil, and is

2   discussed below.

3

4   **4.3 Ground Heat Flux Formulation**

5   The ground heat flux is calculated between every two consecutive soil temperature values

6   in the vertical profile, using both the measured temperatures and the modeled temperatures

7   calculated by Model A and previously shown in Figure 2. The nighttime ground heat flux profile

8   calculated from the modeled temperatures is relatively uniform throughout the soil profile

9   (Figure 4). While it agrees reasonably well with the ground heat flux profile derived from the

10   observations, it is somewhat overestimated above 2 cm. The daytime ground heat flux profile

11   calculated from the modeled temperatures is also relatively uniform throughout the soil profile.

12   However, it is seen to significantly underestimate the ground heat flux profile based on

13   observations above 4 cm.

14   The steep temperature gradient observed during the day (Figure 2) will correspond to an

15   equally strong gradient in G (Figure 4). When calculating G across small intervals, it is highly

16   important that depths, and consequently *dz*, be recorded with maximum accuracy. Even small

17   variations in depth, can result in large differences in the calculated soil heat flux. This, in part,

18   may be a factor in the apparent erratic behavior of the calculated ground heat flux near the soil

19   surface (see Figure 4). However, notwithstanding these observations, the results are consistent

20   with the previous discussion, regarding the underlying assumptions of the Van Wijk Model, and

21   how they implicitly result in a uniform ground heat flux profile.

22   Also included in Figure 4 are the measured net radiation, shown at 0 cm, and the

23   measured ground heat flux at 5 cm depth, indicated by '◊' during the day and 'o' at night. These

1   values are consistent with the ground heat flux profile as calculated from the measured

2   temperatures. This was found to be the case with the Wageningen dataset as well, and suggests

3   the possibility of modeling the ground heat flux profile based only on the net radiation, estimated

4   soil moisture, and an estimate of the ground heat flux at 5 cm. This is explored further in the next

5   section.

6

7   **4.4 Modified Soil Temperature Model (Model B)**

8   As shown previously, model A is not able to describe the near surface temperature

9   fluctuations during periods of high incoming radiation. Another drawback in applying model A

10   is the need for a sufficient number of consecutive temperature measurements that are typically

11   not available at satellite scales. For these reasons a new approach is proposed that is better able

12   to describe the near surface temperatures. The first step consist of generalizing the shape of the

13   instantaneous ground heat flux profile relative to net radiation and the ground heat flux at 5 cm.

14   In the second step, this modeled ground flux profile is used together with the moisture content of

15   the profile to extrapolate the temperature from a single observation depth to a complete surface

16   temperature profile. Because the instantaneous ground heat flux is modeled, no phase correction

17   is needed, making this approach ideally suited for satellite applications that have limited

18   temporal resolution.

19   As described in the previous section, the ground heat flux can be calculated between any

20   two temperature measurements in the vertical profile. From the temperature observations from

21   both the Phoenix and Wageningen field experiments it was found that the shape of the ground

22   heat flux profile can be generalized relative to R_N and an estimated ground heat flux at 5 cm

23   during the day. From theory and field data we know that G approaches R_N at the surface and that

1   below a certain depth, G continues to decrease only slowly with depth (see Figure 4 *day*). The

2   shape of the ground heat flux profile can be described by an S-shaped function

3 $$S(z) = 0.5 \cdot \cos(\pi \cdot z / \alpha) + 0.5 \qquad (10)$$

4

5   where α is the energy transition zone, defined as the depth at which G approaches the total heat

6   flux in the soil, and is strongly related to the moisture content. In our data sets values of α are

7   found between 2 and 5 cm. The parameters are chosen so that S is 1 at the surface and

8   approaches 0 at $z = \alpha$. The ground heat flux can then be expressed as:

9 $$G(z) = R_N \cdot (\beta + (1-\beta) \cdot S) \quad \textit{for daytime} \qquad (11)$$

10   where β is the ratio of G_{5cm}/R_N during the day. If the ratio G_{5cm}/R_N is unknown, it can be

11   estimated at approximately ~0.25. This is slightly less than the average value for the entire day of

12   ~0.3 as found in the literature (Fuchs and Hadas, 1972; Idso et al., 1975; Kustas, 1990), where

13   the ground heat flux was measured at a shallower depth.

14   At night the soil surface loses heat to the atmosphere instead of gaining heat from

15   incoming radiation. The R_N at night does not drive the ground heat flux, but rather is a result of

16   it. Also different processes, such as dew, come into play at night. It is therefore not surprising

17   that the G profile has a different relation with R_N at night. This is shown for the Phoenix field

18   data (see Figure 4 *night*), where it was found that the nighttime G profile starts at approximately

19   1.5 times the R_N at the surface to approximately equal to the R_N at a depth of $z=\alpha$:

20 $$G(z) = R_N \cdot (1 + 0.5 \cdot S) \quad \textit{for nighttime} \qquad (12)$$

21   Because the nighttime fluxes are generally lower, the temperature model is less sensitive to the

22   precise shape of the nighttime ground heat flux profile.

23

1 With G now known, the temperature difference over a soil layer with thickness δz can then be

2 calculated by inverting Equation 2, such that

3
$$\delta T = G \cdot \delta z / \lambda \qquad (13)$$

4 **4.5 Calibration of Modified Soil Temperature Model**

5   The depth of α determines the availability of water for evaporation. When soil moisture

6 is high, the available energy will leave the soil by means of evaporation in a relatively shallow

7 soil layer and α will be small. In a dry soil, evaporation will have to take place over a thicker

8 layer (larger α) in order to create the same latent heat flux.

9   The relationship of α with moisture content is derived from the Phoenix data. The steps

10 for this procedure are outlined in Figure 5. From the measured temperature profile (Figure 5a),

11 we calculate the ground heat flux profile (Figure 5b). Observed values for Rn (shown at 0 cm),

12 and G_{5cm} are indicated with a diamond (1300 hours) and a circle (0100 hours). Next, we model

13 the G profile using observed Rn and G_{5cm} with Eqs. 10–12 (Figure 5c). We then calculate the

14 temperature profile again, based on the temperature at 5 cm and the modeled G profile according

15 to Equation 13 (Figure 5d).

16   The depth of the α parameter is optimized to yield the lowest RMS error for the modeled

17 temperature profile. While the optimized G-profile compares only loosely to the calculated

18 profile (Figure 5c), much of the difference between the two could be accounted for by small

19 variations in the recorded depths. It is extremely difficult to maintain constant and accurate

20 instrument depths, especially near the soil surface. This becomes even more problematic, when

21 the dimensions of the individual sensor exceed that of the depth interval between sensors. A

22 difference in the recorded depth of one of the temperature measurements by as little as one

23 millimeter can result in a significant change in the calculated soil heat flux. Another possible

1 uncertainty may be in the accuracy of the G_{5cm} measurement and its recorded depth. However, in

2 this paper we hold to the data and recorded depths as originally recorded. Nevertheless, the

3 corresponding temperature profile compares well to the measured profile, with an RMS error of

4 1.2 K (Figure 5d).

5 The above procedure was repeated for each measurement day, in order to derive values of

6 the α parameter for all available soil moisture conditions. Figure 6 shows how these optimized α

7 values relate to the soil moisture content (θ) at 0.25 cm. The 0.25 cm depth was chosen because

8 α showed the highest sensitivity for the moisture content at this depth. The relationship between

9 the depth (cm) of the α parameter and moisture content may be described as:

10 $$\alpha = 4.3 - 7.2 \cdot \theta \qquad\qquad for\ \theta > 0.04 \qquad\qquad (14)$$

11 $$\alpha = 4.0 \qquad\qquad for\ \theta < 0.04$$

12 When the soil moisture content is less than 0.04 $m^3 m^{-3}$, the latent heat flux component is

13 extremely small, and results in a large scatter of the thickness of the energy transition zone (α).

14 For these conditions we set α to 4 cm. When this formula is applied to soil moisture depths

15 other then 0.25 cm, best results are achieved when the soil moisture values are within the top

16 centimeter of the soil.

17

18 **4.6 Model B Simulation Results**

19 The new approach is applied to the Phoenix field data, for the same period illustrated

20 previously in Section 4.2, using the average value of β for the entire 14–day experimental period

21 and the calibrated value of α. The 4–day time series of modeled temperatures is shown with both

22 the input observations as well as observations at the modeled depth (Figure 7). The 5 cm to 2 cm

23 and 2 cm to 5 cm simulations are comparable to the previous results, both with RMS errors of

1   0.9 K for the full 14 day period. The RMS for the time of greatest daily deviation is 1.6 K, which

2   is higher than the Model A results. However, the 5 cm to 0.5 cm and 0.5 cm to 5 cm simulations

3   resulted in RMS errors of 1.5 K for the full period, which is a significant improvement over the

4   original Model. Likewise, the RMS errors for the time of greatest daily deviation are

5   significantly reduced to 2.4 K.

6   The performance of model B is compared to model A by calculating the RMS errors

7   between measured and simulated temperatures at all modeled depths for which data is available.

8   The output temperatures are modeled with input temperatures of 5 cm (upward modeling) and

9   0.5 cm (downward modeling). Upward simulations show similar error profiles for both

10   approaches up to about 2 cm with maximum errors of 0.9 K (Figure 8a). Above 2 cm, however,

11   the error profiles diverge considerably, with errors at 0.5 cm of 3.4 K for model A and 1.6 K for

12   model B. In the downward simulations (Figure 8b), both models show low errors of 0.5 K to 1.0

13   K at 1 cm. However, model B errors increase only slightly with depth and are still only 1.6 K at

14   5 cm, while model A errors increase more rapidly to a maximum of 2.4 K at 2 cm and remain

15   above 2.2 K down to 5.0 cm.

16

17   **5. MODEL VALIDATION**

18   To validate the models, they are applied to the Wageningen data described in Section 3.

19   Eight 5-7 day periods are selected with little or no clouds and precipitation, representing a range

20   of soil moisture contents. In the validation of model B, the relationship as derived earlier for the

21   α parameter (Equation 14) was used. For the β ratio, the period average 1300 hour value of the

22   G_{2cm}/Rn measurement is used, and varies between 0.25 and 0.35 over the 8 month experimental

23   period. This compares to the Phoenix average value of $\beta =0.23$.

1   Table 1 shows the eight selected periods, with average water content, β ratio, surface

2   sensor depth, and RMS errors for models A and B. Model A again performs poorly with RMS

3   errors for the period from 1.8 to 7.8 K, with highest values for the driest periods. Model B

4   performs much better with RMS errors for the period in a more acceptable range from 1.0 to 2.6

5   K. Highest RMS values are again associated with the driest periods.

6   In remote sensing applications site specific β ratios will most likely not be available and a

7   constant value will be used. To test the effect of this simplification, the RMS error for model B is

8   calculated using $\beta = 0.25$ as was suggested in Section 4.4. The results are listed in brackets in

9   Table 1. These values are only slightly different from the values with period specific average.

10   This means that model B is not very sensitive to the β ratio and that a value of 0.25 may be used

11   as a first approximation in global studies.

12   The diurnal time series for a wet 5 day period in May and a dry 7 day period in August

13   are illustrated in Figure 9 for the 5 cm to 0.5 cm and 0.1 simulations. Both wet and dry time

14   series of modeled temperatures are shown with both the input observations as well as

15   observations at the modeled depth. The RMS error for the full wet period is 1.0 K and for the

16   dry period 2.1 K. The RMS errors for the time of greatest daily deviation are also low with 0.8 K

17   for the wet period and 3.0 K for the dry period.

18   The error profiles illustrate the comparative performance of the two models (Figure 10

19   for the wet period, Figure 11 for the dry period). Overall, model B errors are significantly lower

20   than those associated with model A. The lowest errors were achieved during wet conditions, and

21   while dry conditions show slightly greater errors, they also show the most significant

22   improvement in model performance. These results give confidence that the new model has

1 validity in a different soil and for a time period that covers meteorological environments

2 differing from a wet spring to a dry summer and fall.

3

5. SUMMARY AND CONCLUSIONS

5 Two field data sets are used to investigate an approach to model instantaneous near-surface soil

6 temperature profiles from a single observation depth. This approach consists of two parts: 1)

7 Deriving an instantaneous soil heat flux profile based on net radiation and the ground heat flux at

8 5cm depth; 2) Then using the modeled ground heat flux profile to extrapolate a single

9 temperature observation to a complete near-surface temperature profile. The first step is sensitive

10 to the soil moisture content of the profile. It is shown that the commonly used solutions to the

11 heat flow equations result in large errors when applied to more extreme variations in temperature

12 that occur near the surface. The reason for this is that the ground heat flux can not be considered

13 constant within the near-surface soil layers, an assumption that is central to Van Wijk's

14 solutions. An error analysis shows that the proposed approach results in RMS errors that are

15 significantly lower compared to the approach based on Van Wijk's solutions. For the maximum

16 depth of 5 cm between input and modeled temperature depth, the errors for the validation data

17 are between 1 and 3 K. While the errors increase gradually with the distance between measured

18 and modeled temperatures, they are still acceptable for many applications, and indicate that the

19 surface processes are reasonably well described. The model results for the validation field data

20 set show that the model functions at a range of soil and meteorological conditions.

1

2   **REFERENCES**

3   Camillo, P., 1989, "Estimating soil surface temperatures from profile temperature and flux

4   measurements". *Soil Science,* **148**: 233-249.

5   Cuaraglia, D., J. Pousa, and L. Pilan, 2001, "Predicting temperature and heat flow in a sandy soil

6   by electrical modeling". *Soil Sci. Soc. Am. J.,* **65**:1074-1080.

7   De Jeu, R., T. Holmes, and M. Owe, 2003, "Deriving Land Surface Parameters from 3 different

8   vegetated sites with the ELBARA 1.4-GHz Passive Microwave Radiometer", *Proc., Int.*

9   *Symp on Remote Sensing, Vol. 5232,* Int. Soc for Optical Engineering, Bellingham, WA.

10   Elias, E., R. Chicota, H. Torriani, and Q. de Jong van Lier, 2004, "Analytical soil-temperature

11   model: correction for temporal variation of daily amplitude. *Soil Sci. Soc. Am. J.,* **68**:784-

12   788.

13   Fuchs, M. and A. Hadas., 1972, The heat flux density in a non-homogeneous bare loessial soil.

14   *Bound. Layer. Meteor.,* **3**:191-200.

15   Idso, S., J. Aase, and R. Jackson, 1975. "Net radiation-soil heat flux relations as influenced by

16   soil water content variations". *Bound. Layer. Meteor.,* **9**:113-122.

17   Jackson, R., 1973, "Diurnal changes in soil water content during drying", In: R.R. Bruce et al.

18   (Eds.) *Field Soil Water Regime.* special pub. 5. Madison, WI. *Soil Sci. Soc. Amer. Proc.,*

19   5,37-55.

20   Johansen, O., 1975. Thermal conductivity of soils. *Ph.D thesis, University of Trondheim,* p. 236.

21   Kustas, W., and C. Daughtry, 1990, "Estimation of the soil heat flux/net radiation ratio from

22   spectral data". *Agricultural and Forest Meteorology,* **49**:205-223.

1   Peters-Lidard, C.D., E. Blackburn, X. Liang, and E.F. Wood, 1998, "The effect of soil thermal

2   conductivity parameterization on surface energy fluxes and temperatures". *J. Atmospheric*

3   *Sciences*, **55**: 1209-1224.

4   Van Wijk, W., and D. de Vries, 1963, "Periodic temperature variations in a homogeneous soil".

5   In: Van Wijk, W.R. (Ed.) *Physics of Plant Environment.* North-Holland Publ. Co.,

6   Amsterdam. pp. 102-143.

1   Figure Captions

2 1. Schematic representation of heat fluxes in the surface layer of the soil. R_N arrives at the

3 surface and gets transmitted downward into the soil (G). In the first few centimeters much of this

4 energy leaves the soil in the form of latent (LE) and sensible (H) heat flux.

5

6 2. Measured soil moisture profiles (a) and measured and modeled temperature profiles (b) at

7 0100 hours (x) and 1300 hours (•) from the Phoenix field data. Modeled temperature profiles

8 according to Model A (heavy lines), are derived from the 8 cm observation.

9

10 3. Time series of measured and simulated soil temperatures for four days in March from the

11 Phoenix field data. The solid lines indicate the modeled temperature according to model A, the

12 dotted lines show the measured input temperatures, dashed lines show the measured temperature

13 at the output depth.

14

15 5. Calculated ground heat flux profiles from measured temperatures at 0100 hours (x) and 1300

16 hours (•) from the Phoenix field data. The ground heat flux profiles based on the model A

17 temperature profiles are shown as heavy lines.

18

19 5. (a) Measured Temperature profiles from the Phoenix field data, at 0100 ('x') and 1300 ('□')

20 hours. (b) Ground heat flux profile as calculated from the previous temperature profile.

21 Measured Rn and G_{5cm} are indicated by '◊' and 'o' for day and night respectively. (c) Modeled

22 ground heat flux profile (heavy lines), compared with G profile derived from temperature

observations. (d) Modeled temperature profiles (heavy lines) derived from the modeled G

profiles, and compared with observations.

6. Optimized values of α for each day of the Phoenix experiment, as a function of the 1300 hour

soil water content at 0.25cm.

7. Four–day time series of measured and simulated soil temperatures from the Phoenix field

experiment. The solid lines indicate the modeled temperature according to model B; the dotted

lines show the measured input temperatures; dashed lines show the measured temperature at the

output depth.

8. Error profiles comparing performance of models A and B in both upward ($z_1 = 5$ cm) and

downward ($z_1 = 0.5$) directions.

9. Four–day time series of measured and simulated soil temperatures from the Wageningen field

experiment for two periods: one with wet and one with dry conditions. The solid lines indicate

the modeled temperature at 0.5 cm (wet) and 0.1 cm (dry) according to model B; the dotted lines

show the measured input temperatures at 0.5 cm; dashed lines show the observations at the

modeled depth.

10. Error profiles comparing performance of models A and B in both upward ($z_1 = 5$ cm) and

downward ($z_1 = 0.5$) directions for the Wet period of the Wageningen experiment.

Configuration: Soil Moisture profile, modeled a, and averaged G.

1

2   11. Error profiles comparing performance of models A and B in both upward (z_1 = 5 cm) and

3   downward (z_1 = 0.1) directions for the Dry period of the Wageningen experiment. Configuration:

4   Soil Moisture profile, modeled a, and averaged G.

Table 1. Results for selected periods of the 2003 Wageningen field experiment. The RMS error between the measured surface temperature and the modeled value for model A and B are shown, for both the entire period and for the 1300 hour value. For model B, the RMS error in brackets reflects a constant β ratio of 0.25. Shaded periods are illustrated in Figure 9.

| | | | | | Modelled Surface Temperature Errors | | | |
| | | | | | RMS Period (K) | | RMS at 1300 hour (K) | |
Period	Dates	Avg. Wc (cm³/cm³)	Avg. β (-)	Surface sensor depth (cm)	A	B	A	B
1	12-18 April	0.2	0.31	0.5	3.6	2.5 (2.6)	5.4	0.6 (1.1)
2	7-11 May	0.37	0.29	0.5	1.8	1.0 (1.1)	3.4	1.0 (1.5)
3	30 May - 4 June	0.32	0.27	0.5	2.5	1.4 (1.5)	5.0	2.8 (3.0)
4	8-15 July	0.06	0.26	0.3	4.2	2.3 (2.3)	8.5	3.2 (3.1)
5	28 July-3 Aug	0.06	0.26	0.1	6.2	2.1 (2.1)	11	1.5 (1.4)
6	6-9 Aug	0.04	0.28	0.1	7.8	2.2 (2.2)	15	3.0 (3.2)
7	15-21 Sept	0.03	0.36	0.1	6.2	2.7 (3.0)	11	3.1 (4.1)
8	2-5 Oct	0.09	0.26	0.1	2.2	1.6 (1.5)	2.8	2.0 (1.9)
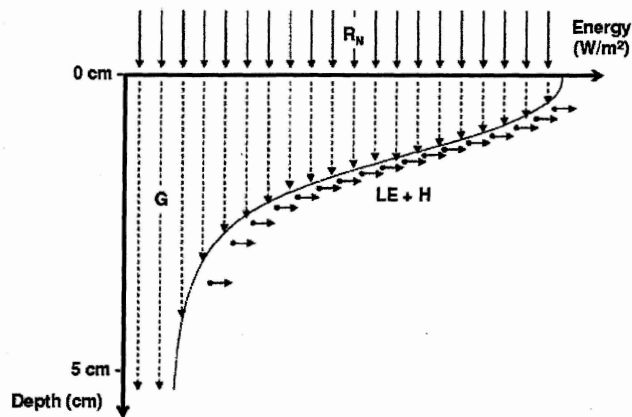
Figure 1: Schematic representation of heat fluxes in the surface layer of the soil. R_N arrives at the surface and gets transmitted downward into the soil (G). In the first few centimeters much of this energy leaves the soil in the form of latent (LE) and sensible (H) heat flux.
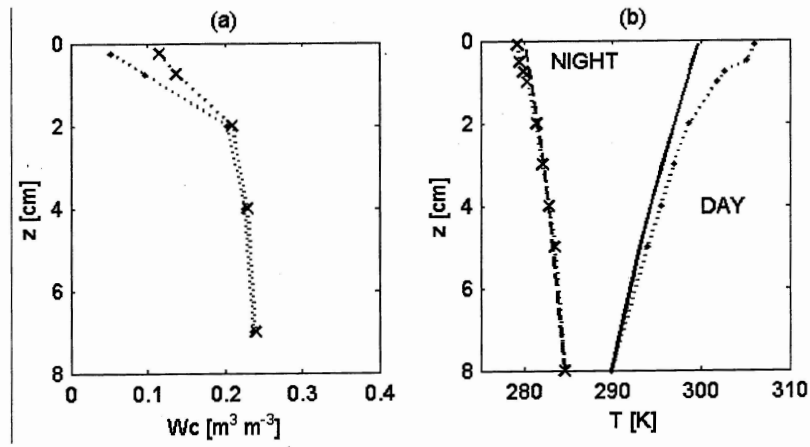
Figure 2. Measured soil moisture profiles (a) and measured and modeled temperature profiles (b) at 0100 hours (x) and 1300 hours (•) from the Phoenix field data. Modeled temperature profiles according to Model A (heavy lines), are derived from the 8 cm observation.
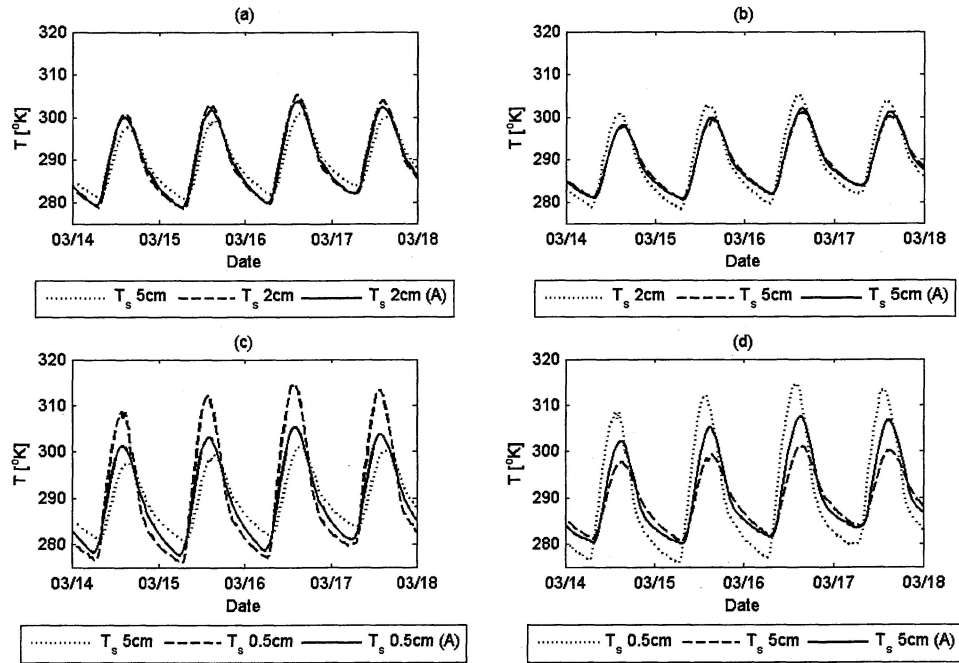
Figure 3: Time series of measured and simulated soil temperatures for four days in March from the Phoenix field data. The solid lines indicate the modeled temperature according to model A, the dotted lines show the measured input temperatures, dashed lines show the measured temperature at the output depth.
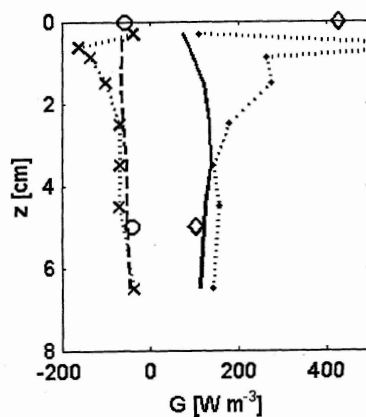
Figure 4. Calculated ground heat flux profiles from measured temperatures at 0100 hours (x) and 1300 hours (•) from the Phoenix field data. The ground heat flux profiles based on the model A temperature profiles are shown as heavy lines.
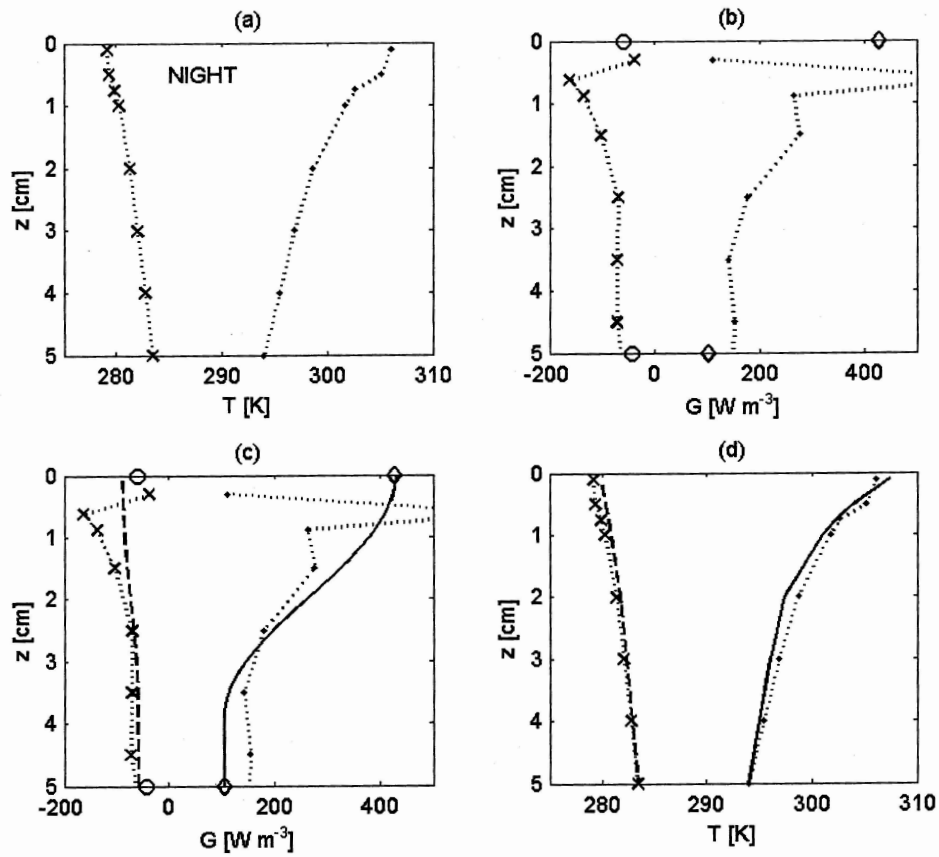
Figure 5: (a) Measured Temperature profiles from the Phoenix field data, at 0100 ('x') and 1300 ('□') hours. (b) Ground heat flux profile as calculated from the previous temperature profile. Measured Rn and G_{5cm} are indicated by '◊' and 'o' for day and night respectively. (c) Modeled ground heat flux profile (heavy lines), compared with G profile derived from temperature observations. (d) Modeled temperature profiles (heavy lines) derived from the modeled G profiles, and compared with observations.
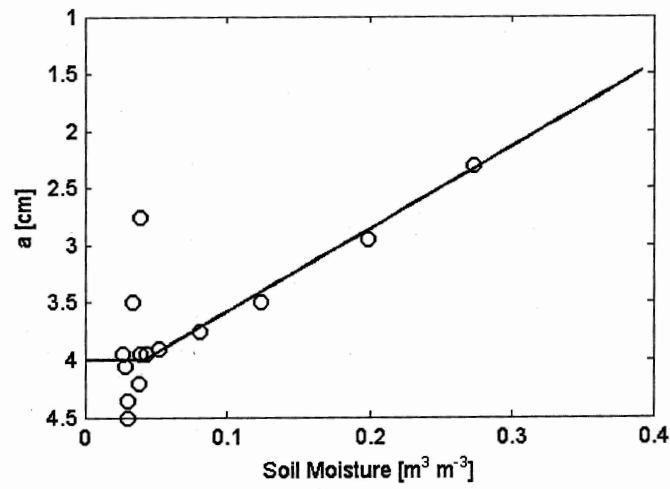
Figure 6. Optimized values of α for each day of the Phoenix experiment, as a function of the 1300 hour soil water content at 0.25cm.
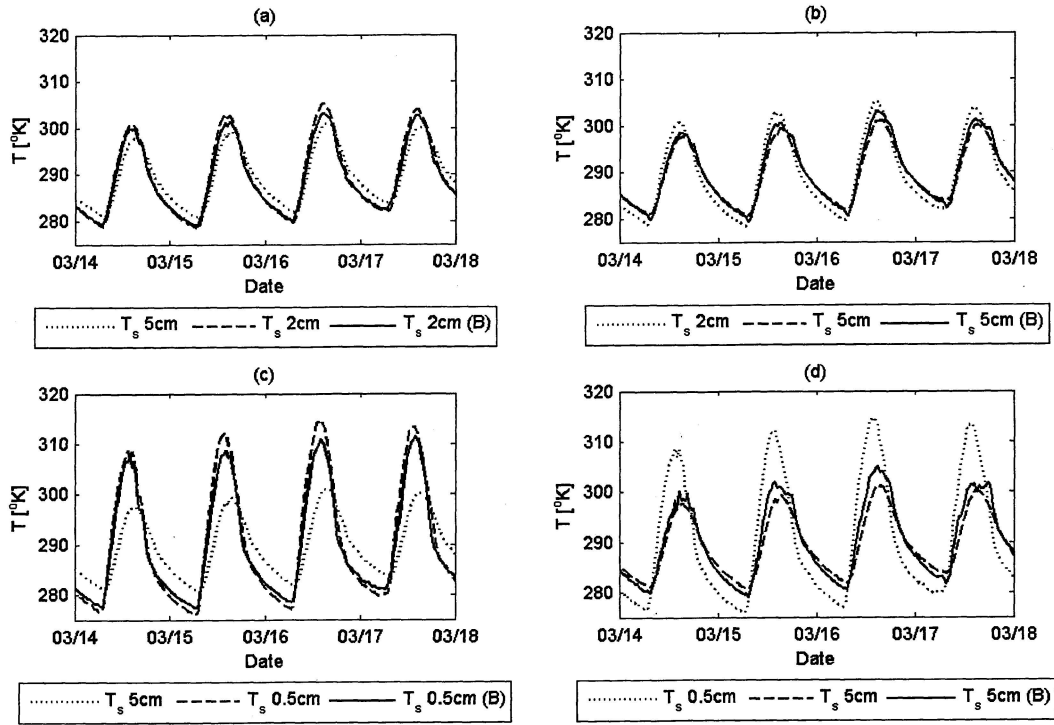
Figure 7: Four–day time series of measured and simulated soil temperatures from the Phoenix field experiment. The solid lines indicate the modeled temperature according to model B; the dotted lines show the measured input temperatures; dashed lines show the measured temperature at the output depth.
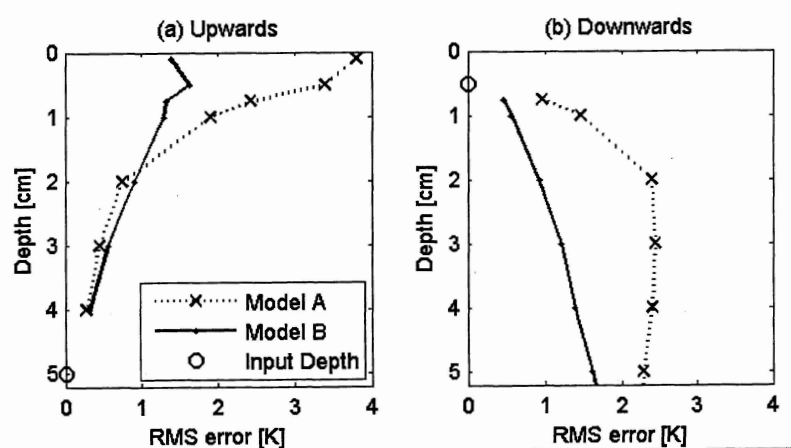
Figure 8. Error profiles comparing performance of models A and B in both upward ($z_1 = 5$ cm) and downward ($z_1 = 0.5$) directions.
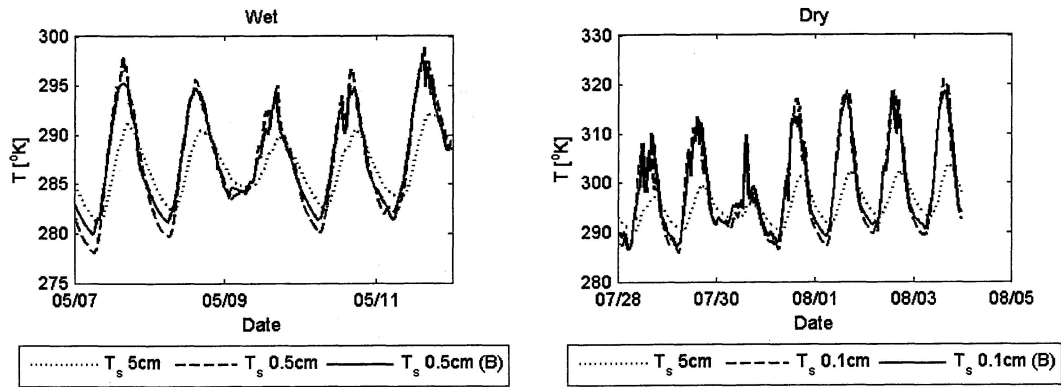
Figure 9. Four–day time series of measured and simulated soil temperatures from the Wageningen field experiment for two periods: one with wet and one with dry conditions. The solid lines indicate the modeled temperature at 0.5 cm (wet) and 0.1 cm (dry) according to model B; the dotted lines show the measured input temperatures at 0.5 cm; dashed lines show the observations at the modeled depth.
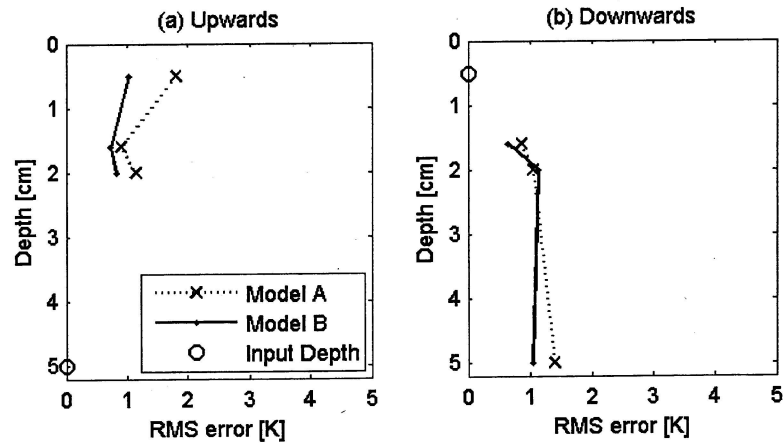
Figure 10. Error profiles comparing performance of models A and B in both upward $(z_1 = 5$ cm) and downward $(z_1 = 0.5)$ directions for the Wet period of the Wageningen experiment. Configuration: Soil Moisture profile, modeled a, and averaged G.
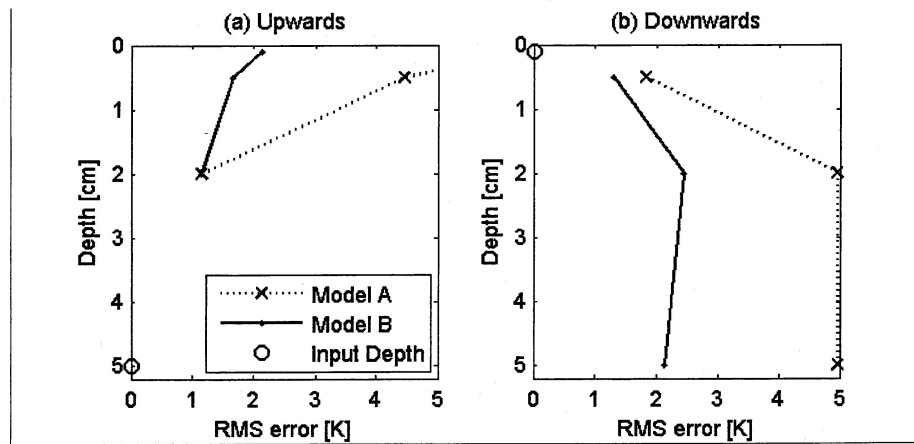
Figure 11. Error profiles comparing performance of models A and B in both upward ($z_1 = 5$ cm) and downward ($z_1 = 0.1$) directions for the Dry period of the Wageningen experiment. Configuration: Soil Moisture profile, modeled a, and averaged G.